On structural features of fullerene C-60 dissolved in carbon disulfide: Complementary study by small-angle neutron scattering and molecular dynamic simulations

ARTICLE *in* THE JOURNAL OF CHEMICAL PHYSICS · APRIL 2010

Impact Factor: 2.95 · DOI: 10.1063/1.3415500 · Source: PubMed

On structural features of fullerene C_{60} dissolved in carbon disulfide: Complementary study by small-angle neutron scattering and molecular dynamic simulations

M. V. Avdeev,[1,a)] T. V. Tropin,[1] I. A. Bodnarchuk,[2] S. P. Yaradaikin,[1] L. Rosta,[3] V. L. Aksenov,[1,4] and L. A. Bulavin[5]
[1]*Frank Laboratory of Neutron Physics, Joint Institute for Nuclear Research, 141980 Dubna Moscow Reg., Russia*
[2]*Skobel'tsyn Institute of Nuclear Physics, Moscow State University, 119991 Moscow, Russia*
[3]*Research Institute for Solid State Physics and Optics, Hungarian Academy, 1525 Budapest, Hungary*
[4]*Russian Research Center "Kurchatov Institute", 123182 Moscow, Russia*
[5]*Taras Shevchenko National University of Kyiv, 03022 Kyiv, Ukraine*

(Received 10 September 2009; accepted 6 April 2010; published online 28 April 2010)

The parameters of fullerene C_{60} dissolved in carbon disulfide CS_2 are analyzed by small-angle neutron scattering (SANS) in a wide interval of momentum transfer. To exclude the influence of nonequilibrium conditions, the solutions are prepared without applying shaking, stirring or ultrasound. No indication of the equilibrium cluster state of C_{60} (with the cluster size below 60 nm) in the final solutions is revealed. Molecular dynamic simulations are complementary used to find out the partial volume of C_{60} in CS_2 and the scattering contribution of the solvent organization at the interface with the fullerene molecule, which is shown to be small. Among several approaches for describing SANS data the preference is given to the model, which takes into account the presence of stable C_{60} dimers (comprising 10% of the total particle number density) in the solution.
 [doi:10.1063/1.3415500]

I. INTRODUCTION

Among allotropic forms of carbon only fullerenes (stable and highly symmetric molecules C_{60}, C_{70}, etc.) are soluble in a number of organic and nonorganic solvents.[1–3] The corresponding solutions are often characterized as of molecular type with the solubility limits. However, some specific features of these systems distinguish them from purely molecular solutions. In particular, it concerns a tendency of dissolved fullerenes (size of about 1 nm) to form clusters in different conditions.[3,4] The fullerene clusterization correlates at some extent with the solvent polarity, so it certainly takes place in quite polar solvents such as pyridine,[5] N-methyl-pyrrolidone,[6] benzonitrile,[7] and alcohols.[5,7,8] For low-polar solvents the literature data are sometimes contradictory.[9] Thus, the densitometry value of the specific partial volume of the C_{60} molecule in toluene and carbon disulfide (CS_2) coincides well with its Van der Waals volume.[10] The rheological measurements confirm the molecular state of C_{60} in decalin.[11] At the same time, fullerene clusters were observed in benzene by dynamic light scattering[7,12–14] and in toluene by small angle-neutron scattering (SANS).[15] Also, the formation of large fullerene clusters up to 100 nm in size was detected for the C_{60} solutions in carbon disulfide by photon correlation technique and electron microscopy.[16] The possible appearance of large clusters, which can precipitate from the solution, was used[17] for explaining the complex kinetics of fullerene dissolution in CS_2 reflected in the time dependence of the fullerene concentration as a slight peak at the time scale of one month after the preparation.[10] Smaller clusters (size of about 6 nm) composed of a small part (about 10%) of the dissolved fullerene molecules in this solution were observed[18,19] by SANS. Finally, the existence of stable dimers of C_{60} in chlorobenzene was concluded from the vapor pressure osmometry;[20] the same was proposed[18,19] for solutions of C_{60} in carbon disulfide to explain larger apparent size of fullerene molecules revealed by SANS.

The appearance of clusters was related[3] to a peak in the temperature dependence of the C_{60} solubility[21] in a number of low-polar solvents (hexane, toluene, carbon disulfide, and xylene); as a result, the equilibrium cluster model for fullerene solubility was developed.[3] It should be mentioned that the alternative model explaining this peculiarity is based[22,23] on the transition of the solid phase in saturated solutions into solvatocrystals, which changes the equilibrium and, consequently, the solubility of fullerene depending on temperature.

In the present work we consider the possible effect of the cluster formation in solutions of C_{60} in carbon disulfide on SANS curves. The SANS curves are obtained in the most possible q interval of $0.1-5\ \mathrm{nm}^{-1}$ for such small molecule. The low incoherent background, comparatively high fullerene solubility in CS_2 (7.9 mg/ml) and sufficient contrast [mean neutron scattering length density (SLD) above $4\times10^{10}\ \mathrm{cm}^{-2}$ for C_{60} against $1.22\times10^{10}\ \mathrm{cm}^{-2}$ for CS_2] allowed us to perform such experiments for reasonable exposition time. Two aspects are concerned. First, the existence of the clusters with size of 10 nm and higher in equilibrium solutions is checked out. An important feature in the reported

a)Electronic mail: avd@nf.jinr.ru.

preparations of the fullerene solutions is that starting from Ruoff *et al.*[1,21] these solutions are often prepared using comparatively intensive sonication for accelerating the procedure. It was concluded by Beck[9] that the nonequilibrium conditions could affect strongly the dissolution process regarding the possible cluster formation. Here, we focus our studies on the C_{60}/CS_2 solutions prepared in equilibrium conditions, i.e., after the fullerene powder is added into the solvent the mixture is left intact (no shaking, stirring or ultrasound were applied) at constant temperature during some time, which is sufficient for self-dissolution of the fullerene. The second aspect of the work is related to the effect of small clusters (dimers, trimers, etc.) mentioned above. In addition to the previous interpretations[18,24–29] of the SANS curves from C_{60}/CS_2 solutions the data of the molecular dynamics simulation (MDS) are involved. MDS was performed for the interface C_{60}/CS_2 in a way similar to the work of Malaspina *et al.*,[30] where the C_{60} interface in the ethanol solution was revealed by MDS. The partial fullerene volume is estimated; and atomic displacements provided by MDS are used for calculation of the neutron SLD in the vicinity of the fullerene surface. The almost spherical symmetry of the C_{60} molecule gives a unique possibility to make the analysis in terms of isotropic SLD distribution about the center-of-mass of C_{60}.

II. METHODS

Preparation of solutions. Solutions of fullerene C_{60} (purity 99.5%, Fullerene Technologies, St. Petersburg) in carbon disulfide (purity 99.98%, Merck) were prepared in the following way. The fullerene powder was added to the solvent and left intact for about 55 h at a temperature of 20 °C. Any mechanical actions (shaking, stirring, and ultrasound treatment) were avoided. Two samples with the effective concentrations of 4.08 and 7.90 mg/ml as calculated from the mass of the added powder and solvent volume were studied. Below these solutions are conventionally referred to as nonsaturated and saturated samples.

SANS. SANS experiments (nonpolarized mode) were performed on the small-angle instrument "Yellow Submarine" at the Budapest Neutron Center (BNC). The differential cross section per sample volume (scattering intensity) isotropic over the radial angle φ on the detector plane was obtained as a function of the momentum transfer module, $q=(4\pi/\lambda)\sin(\theta/2)$, where λ is the incident neutron wavelength and θ is the scattering angle. Measurements were made at a fixed neutron wavelengths of 0.34 and 0.61 nm (monochromatization full width at half maximum $\Delta\lambda/\lambda=13\%$) and sample-detector distances of 1.3 and 5.5 m (detector size 64 cm) to cover a q range of $0.01\div0.5$ Å^{-1}. A standard procedure to calibrate the cross section on a water sample of 1 mm thick[31] together with the corrections on the background, container scattering and incoherent background (subtraction of the scattering from pure solvent) was performed. The samples and the pure solvent were put into quartz cells (Hellma) of 5 mm thick and were kept at room temperature (20 °C) during the expositions. Each curve was obtained for about 15 h including measurements of the solvent scattering.

MDS. The MD simulations were carried out on the parallel PC cluster of the Laboratory of Information Technologies in the Joint Institute for Nuclear Research with the simulation code DL_POLY_2.18.[32] The intermolecular interaction in solution was modeled with the sum of the Lennard-Jones potentials with the cutoff radius of 10 Å and the Coulombic potential with cutoff radius of 25 Å

$$U=\sum_{ij}4\varepsilon_{ij}\left[\left(\frac{\sigma_{ij}}{r_{ij}}\right)^{12}-\left(\frac{\sigma_{ij}}{r_{ij}}\right)^{6}\right]+\frac{q_iq_j}{r_{ij}}, \quad (1)$$

where σ_{ij} and ε_{ij} are the parameters of the Lennard-Jones interaction between atoms i and j positioned at the distance r_{ij} between them; q_i and q_j are their charges. The parameters of interaction between nonidentical atoms were found according to the standard Lorentz–Berthelot combination rule[33]

$$\sigma_{ij}=(\sigma_{ii}+\sigma_{jj})/2, \quad (2a)$$

$$\varepsilon_{ij}=\sqrt{\varepsilon_{ii}\varepsilon_{jj}}. \quad (2b)$$

For CS_2 we used[34,35] $\sigma_{CC}=3.35$ Å, $\varepsilon_{CC}=0.1016$ kcal/mol and $\sigma_{SS}=3.52$ Å, $\varepsilon_{SS}=0.3633$ kcal/mol, $q_C=-0.308e$ and $q_S=0.154e$. The Ewald algorithm was applied to treat the long-range CS_2-CS_2 electrostatic interactions. For the interactions between atoms of fullerene and the solvent we used (2) with the Lennard-Jones parameters of C_{60} in the crystalline state, which are[25] $\sigma_{CC}=3.47$ Å, $\varepsilon_{CC}=0.0660$ kcal/mol.

CS_2 molecules were considered as rigid units with the bond length of 1.55 Å between carbon and sulfide atoms.[36] The fullerene C_{60} was considered as the rigid unit with the bond lengths[37,38] of 1.39 and 1.44 Å, and radius of 3.55 Å known from x-ray diffraction.[39] The SHAKE algorithm was employed to constrain the bond lengths. First, the simulations were performed for pure solvent CS_2 in the cubic cell containing 4096 molecules. The cubic periodical boundary conditions were used. The system was relaxed in the Nose–Hoover NPT ensemble (constant particle number, atmospheric pressure and temperature 293 K, the relaxation time constant of barostat and thermostat is 0.3 ps). Then, one C_{60} molecule was placed in the center of the cell. The CS_2 molecules coordinately overlapped with fullerene atoms were removed, so the resulting number of CS_2 was 4069 molecules per one fullerene. The system relaxation was repeated under the same conditions up to the local equilibrium state (during 20 ps) and then atomic coordinates were recorded every 0.1 ps in 6.0 ns trajectory. The step of integration of motion equations in both cases was 0.001 ps.

III. RESULTS AND DISCUSSION

A. SANS. Guinier analysis

SANS curves obtained for the two solutions are given in Fig. 1. As it was proved previously,[24] despite a rather small signal, the scattering can be reliably connected with the dissolved fullerene molecules. The double logarithmic representation shows well the Guinier peculiarities corresponding to the size of about 1 nm. The linear fits to the experimental data in the Guinier coordinates [$\ln(I)$ versus q^2] are demonstrated in the inset. The resulting values of the radius of gyration R_g are 3.85 ± 0.18 and 3.84 ± 0.17 Å for nonsat-

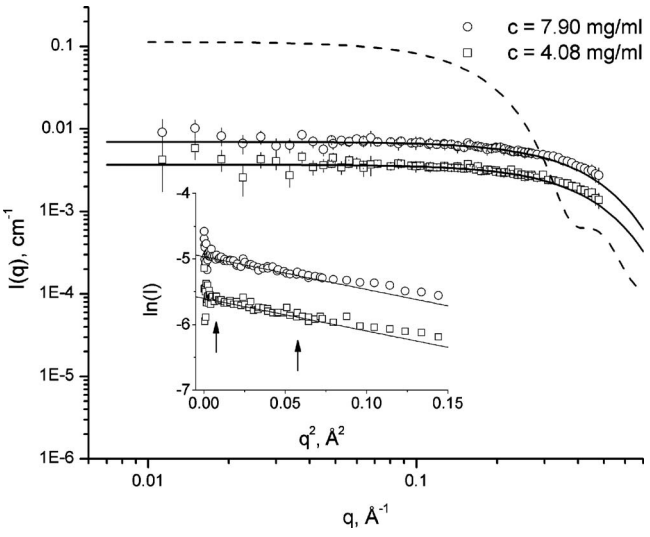

FIG. 1. Experimental SANS curves (points) for two solutions of fullerene C_{60} in CS_2 with different solute concentration, c. Dashed line shows the curve calculated for solution with $c=7.90$ mg/ml according to the cluster model [3]. Solid lines correspond to the Guinier approximations; systematic deviation at large q values can be seen. Inset shows the Guinier plots of the experimental curves (points) and corresponding linear approximations. Arrows indicate the interval used for the linear approximation ($R_g q<0.9$).

urated and saturated samples, respectively, and satisfy the condition $qR_g<1$ for the used interval (denoted in inset to Fig. 1). The obtained R_g value agrees well with the range of 3.7–3.9 Å, which covers values found in the previous SANS experiments.[18,24–29] The ratio between $I(0)$ values, 0.0070(1) cm^{-1}/0.0037(1) cm^{-1}=1.89(6), determined from the Guinier approximation for the two samples coincides within the error with the corresponding concentration ratio, 1.93, thus testifying that all of the fullerene added to the solvent is dissolved and that there is no significant structure-factor effect in the studied system. The last statement repeats the earlier conclusion[27] and justifies the way the MDS is performed, when only one fullerene molecule is placed into the model solvent cell (infinite dissolution). It is worth mentioning that the cross section per volume from CS_2 itself obtained after the empty cell correction is 0.0022(5) cm^{-1}, i.e., the forward scattering from the fullerene solution with the lower concentration exceeds more than 1.5 times the solvent scattering.

The resolution effects in this case are negligibly small. In accordance with estimates by different algorythms[40–42] the corresponding shift in the obtained parameters for the Gunier approximation is significantly below 1%. The indirect Fourier transform with the GNOM program[43] gives one R_g value of 3.77 ± 0.07 Å for both samples, which coincides well with the radii obtained by the Guinier approximation. The relative error of the Guinier approximation can be estimated using the equation[44]

$$\frac{\Delta R_g}{R_g}\approx\frac{3M_2M_6-5M_4^2}{360M_2^2}\mu^4(qR_g)^4, \tag{3}$$

where $\mu=D/R_g$; M_k is the normalized kth moment of the particle correlation function $\gamma(r)$

$$\gamma(r)=\frac{1}{2\pi^2}\int_0^\infty I(q)\frac{\sin qr}{qr}q^2dq, \tag{4a}$$

$$M_k=\int_0^1 x^k\gamma(xD)dx. \tag{4b}$$

From (3) and (4) for a homogeneous sphere and $qR_g<1$ the deviation from the Guinier law is about 1%.

The important observation at this stage of the analysis is that there is no obvious effect of clusterization at smallest q values like in the solutions prepared under strongly nonequilibrium conditions.[18,19] Also, the SANS data do not support the prediction of the cluster model for fullerene solutions developed[3] to explain the peak in the temperature dependence of the C_{60} solubility. This follows from the comparison (Fig. 1) of the experimental curve for the saturated sample with the model curve calculated with the size distribution function from the cluster model[3] assuming the spherical cluster shape. However, the existence of very large clusters, which explain[17] the time dependence of the total C_{60} concentration in the solution within one month after preparation,[10] cannot be excluded. Particularly, it can be reflected in some positive deviation of the scattering from the Guinier law at the smallest q values in the inset to Fig. 1. The characteristic size of such clusters (above 60 nm) is estimated from the resolution limit of the given experiment in accordance with the rule $q\sim2\pi/D$ (where D is the particle size) by using the minimal measured q value.

B. MDS

The MDS data were treated in terms of the radial distribution function (RDF), $g(\vec{r})$, which shows the time-averaged influence of one atom on the disposition of neighboring atoms. By definition, the probability to find some atom in a liquid at the distance $\vec{r}$ from an arbitrary fixed atom is[33]

$$\rho g(\vec{r})=\frac{1}{N}\left\langle\sum_i^N\sum_{j\neq i}^N\delta[\vec{r}-\vec{r}_{ij}]\right\rangle, \tag{5}$$

where N is the total number of atoms in the simulation cell; $\rho=N/V$ is the number density of atoms; $\vec{r}_{ij}$ is the vector between the centers of ith and jth atoms; and brackets $\langle\ldots\rangle$ denote averaging over time. The $g(\vec{r})$ function is defined in a way that for distances less than one atomic diameter $g(\vec{r})=0$, and for large distances in liquid where one atom does not influence the disposition of others $g(\vec{r})=1$. For isotropic liquids Eq. (5) is averaged over the whole space angle, so that RDF is a function of the scalar r, $g(r)$. The $g(r)$ function was analyzed in a standard way, when partial RDFs corresponding to correlations of the types C–C, S–S, and C–S are compared.

RDFs for pure CS_2 calculated by MDS (6 ns period) are shown in Fig. 2. They are in a good agreement with the functions found experimentally and using MDS by other research groups.[34,35,45,46] From the given simulation the CS_2 density is found to be 1.265 ± 0.004 g cm^{-3}, which repeats well the tabular value of 1.260 g cm^{-3}.

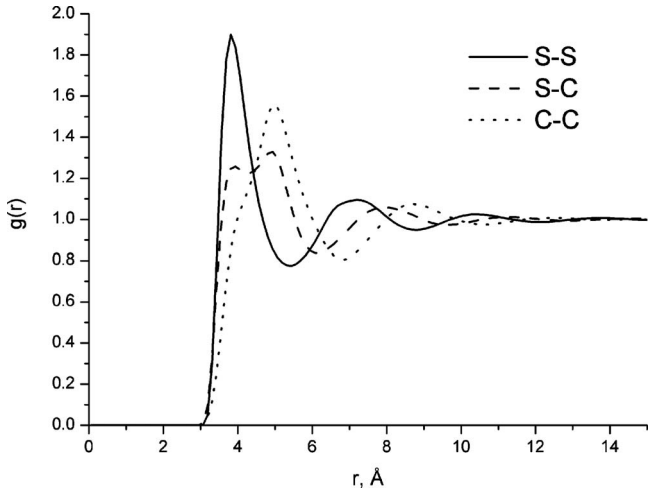

FIG. 2. Partial radial distribution functions in neat CS_2 calculated by MDS.

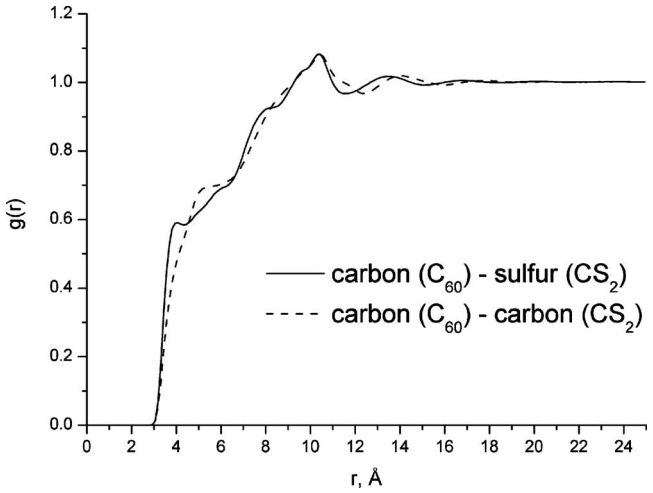

FIG. 4. Solute-solvent radial distribution functions calculated by MDS.

After the simulation starts with the C_{60} molecule in the model cell as described above, the equilibrium state is achieved for less than 5 ps. This estimate follows from the time dependence of the model cell volume (Fig. 3), V, which finally oscillates near the average value of $409\,000 \pm 1200$ Å^3. The limit partial volume, $\bar{V}^{\infty}$, of the fullerene is found from the partial solute-solvent atomic RDFs plotted in the same way as for isotropic pure CS_2 (Fig. 4). By definition, $\bar{V}^{\infty}$ is the difference between the solute volume and solvent volume in it in the case of the infinitely large solvent cell (interaction between solute molecules is entirely excluded). If the cutoff boundary around the solute $|\vec{r}|=\lambda$, beyond which the solvent properties would equal their asymptotic limit, then the λ-dependent value of $\bar{V}^{\infty}(\lambda)$ can be found from the expression[47,48]

$$\bar{V}^{\infty}(\lambda) = \frac{\int_{|\vec{r}|<\lambda}(1-g(\vec{r}))d\vec{r}}{1-\frac{1}{V}\int_{|\vec{r}|<\lambda}g(\vec{r})d\vec{r}} = \frac{\int_{r<\lambda}4\pi r^2(1-g(r))dr}{1-\frac{1}{V}\int_{r<\lambda}4\pi r^2 g(r)dr}, \quad (6)$$

where $g(\vec{r})$ is any solute-solvent atomic RDF. In Fig. 5 the dependence $\bar{V}^{\infty}(\lambda)$ calculated on the basis of two solute-solvent RDFs as a function of integral cutoff λ is given. One can see that the volume $\bar{V}^{\infty}$ converges rapidly in the two cases to its asymptotic value of 690 ± 4 Å^3 with the corresponding radius of 5.48 ± 0.01 Å. The error is the consequence of the time-dependent dynamics of fullerene volume in solution because of the equilibrated motion of molecules in the model cell resulting in time fluctuations of the solute-solvent RDFs. These fluctuations are significant in the beginning of the MD simulation but are steeply smoothed with the averaging over a great number of different configurations, so that after 4 ns the error is less than 1%. The found excluded volume $\bar{V}^{\infty}$ is significantly larger than the van der Waals volume[6,28] (530 Å^3) with the corresponding radius of 5.02 Å of a single C_{60} in the crystalline state calculated from the x-ray diffraction data.[39] It should be noted that the possible effect of C_{60} vibrations on the molecular volume determined by MDS (nonrigid model) was considered[30] for C_{60}/ethanol solution and found to be negligibly small.

Then, the MDS data were used for calculating the SLD distribution $\rho(r)=(\Delta b/4\pi r^2\Delta r)$ around the fullerene molecule, where r is measured from the fullerene center-of-mass

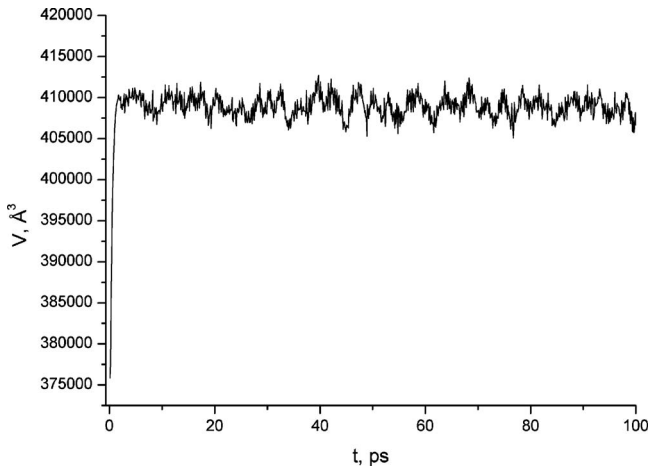

FIG. 3. The dynamics of solute volume during the relaxation in NPT ensemble at atmospheric pressure and 293 K.

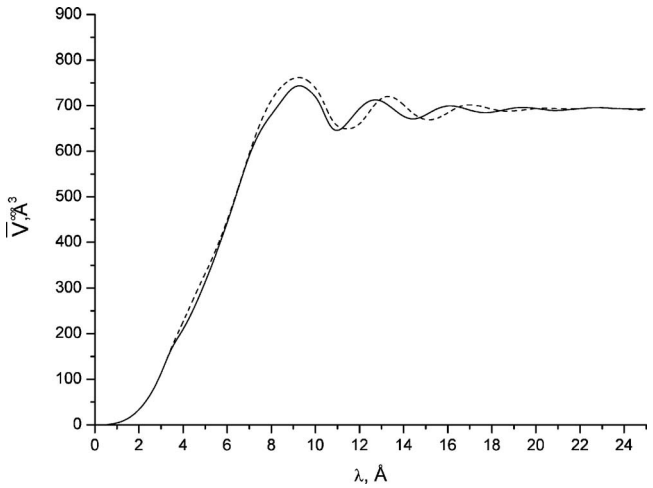

FIG. 5. Fullerene limit partial volume $\bar{V}^{\infty}$ as a function of integral cutoff λ calculated from RDF carbon of C_{60}—sulfur of CS_2 (solid line) and carbon of C_{60}—carbon CS_2 (dashed line).

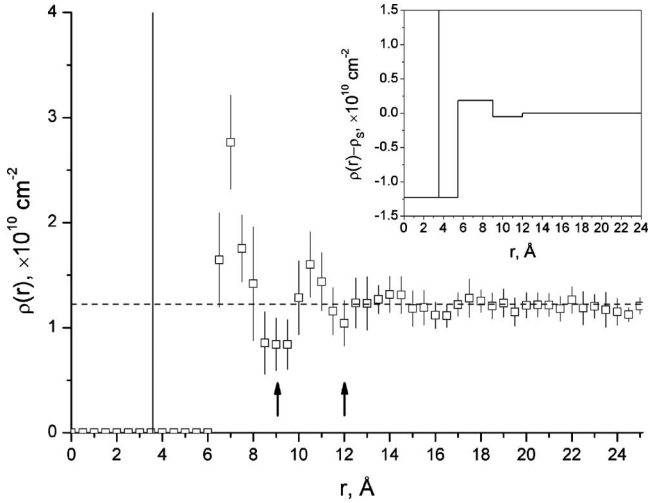

FIG. 6. The neutron SLD of the solute, $\rho(r)$, calculated from the center of fullerene with $\Delta r=0.5$ Å. The peak at $r=3.55$ Å shows the δ-function corresponding to the distribution of C nuclei in C_{60}. The dashed line shows bulk SLD, ρ_s, of pure CS_2. The arrows mark the boundary of the first and second coordination spheres at the interface C_{60}/CS_2. The inset shows the effective neutron SLD profile of the solvated fullerene against the SLD of bulk solvent (contrast), $\rho(r)$-ρ_s.

and Δb is the total scattering length per the spherical shell of the thickness Δr. The resulting $\rho(r)$ obtained after averaging over nine independent MDS configurations with the step $\Delta r=0.5$ Å is shown in Fig. 6. Since neutrons are scattered by atomic nuclei, one can see a large narrow peak at $r=3.55$ Å corresponding to C atoms in the fullerene molecule. Some oscillations reflecting short-range ordering in the solvent at the fullerene interface can be seen. At sufficiently large r values the $\rho(r)$ function approaches a constant corresponding to the bulk solvent SLD, $\rho_S=1.225\times10^{10}$ cm^{-2}, which agrees well with the value of 1.220×10^{10} cm^{-2} calculated from the tabular scattering lengths of atoms in CS_2 and its mass density. The SLD modulation at the C_{60} interface is mainly determined by the two first coordination spheres (indicated by the arrows in Fig. 6) with the approximate thickness of 3 Å each. The number of CS_2 molecules in the first sphere is 25 ± 1, which is less than 32 for ethanol solution.[30] It should be noted that in contrast to C_{60}/CS_2, for the ethanol solution up to four coordination spheres constituting the density fluctuations at the interface are resolved. The found number of CS_2 molecules in the first coordination sphere coincides well with that for the solvation shell proposed[28] for interpretation of the R_g value in the C_{60}/CS_2.

C. SANS modeling

The effective core-shell SLD profile from the MDS data, which are used in the following model calculations, is shown in the inset to Fig. 6. The C-nuclei sphere of C_{60} is represented by δ-function. The fullerene cage including the electron distribution (which has no effect on the neutron scattering) has negative contrast. One can see that from the viewpoint of neutron scattering the fullerene volume with the corresponding radius of 6 Å is higher than that obtained in MDS. This is related to the fact that the distribution of

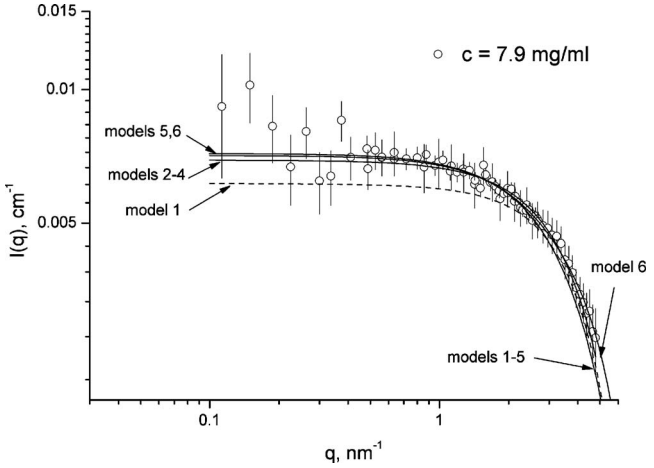

FIG. 7. SANS models (see text) are compared with the experimental curve from the solution with higher concentration.

atomic nuclei in the solvent shifts by approximately atomic Van der Waals radii from the fullerene surface.

The model scattering amplitude corresponding to the isotropic SLD profile in the inset to Fig. 6 is described by the formula

$$F(q) = (4\pi/3)(60b_C \sin(qR_C)/(qR_C) - \rho_s R_0^3 \Phi(qR_0) + (\rho_1 - \rho_s)(R_1^3\Phi(qR_1) - R_0^3\Phi(qR_0)) + (\rho_2 - \rho_s)(R_2^3\Phi(qR_2) - R_1^3\Phi(qR_1))), \quad (7)$$

where $\Phi(x)=3(\sin x - x\cos x)/x^3$; $b_C=0.665\times10^{-12}$ cm is the scattering length of carbon; $R_C=3.55$ Å is the radius of carbon shell in fullerene; $R_0=6$ Å is the radius of fullerene; $R_1=9$ Å, $R_2=12$ Å are the outer radii of the two shells, respectively; and, in addition to the introduced above ρ_s, the densities $\rho_1=1.41\times10^{10}$ cm^{-2} and $\rho_2=1.17\times10^{10}$ cm^{-2} correspond to SLDs of the shells. The first term in (7) corresponds to the carbon sphere in fullerene with the δ-function distribution. The model scattering intensity

$$I(q) = nF^2(q), \quad (8)$$

where n is the number particle density, is compared to the experimental data in Fig. 7 for the sample with higher concentration. It is referred as *model 1* in the figure. The resolution function[41] is taken into account. The significant deviation toward lower intensity is revealed. The corresponding radius of gyration found from the SLD distribution using the definition

$$R_g^2 = \frac{\int(\rho(r)-\rho_s)r^2 d\vec{r}}{\int(\rho(r)-\rho_s)d\vec{r}}, \quad (9)$$

gives 2.91 Å, which is also significantly lower than the experimental value. The SLDs of the shells can be specified by fitting Eq. (8) to the experimental curves using (7) with the fixed radii R_0, R_1, and R_2. The resulting curve (*model 2*) is shown in Fig. 7. It gives $\rho_1=(1.33\pm0.15)\times10^{10}$ cm^{-2} and $\rho_2=(1.23\pm0.05)\times10^{10}$ cm^{-2}, which means that for better consistency the effect of the shells can be omitted. The reason is related to the fact that the mean SLD of the two-shell structure does not differ much from the solvent SLD, thus

the small contrast of the whole shell results in a low signal from the shell at $q \to 0$. Still, the corresponding radius of gyration of the discussed model, $R_g < 3.61$ Å, is below the experimental value from the Guinier plot, so the main interval, which is described by the used model, covers large q values (beyond the Guinier region). In this connection the experimental data can be fitted effectively with the model, where the solvent shells are neglected (i.e., $\rho_1 = \rho_2 = \rho_s$), and the radius R_0 is varied. Such model (*model 3*) gives almost the same fitting curve like in the previous case with the effective radius of fullerene $R_0 = (5.2 \pm 0.4)$ Å and corresponding radius of gyration (3.5 ± 0.3) Å. Following the works of Gripon *et al.*[26] and Melnichenko *et al.*[27] the form factor of the fullerene can be reduced to the scattering from only the carbon sphere [the term with $\sin(qR_C)/(qR_C)$ in (7)] with varying R_C (*model 4*). Again, the fitting curve is very close to the two curves above, and gives $R_C = (3.5 \pm 0.1)$ Å, which coincides well with the real R_C, but does not explain the higher value of the measured R_g. So, we can see that there are several models, which fit well the whole curves, but with some deviation from the experimental data in the Guinier region. Henderson supposed[28] that this discrepancy can be explained by the solvation shell of 24 solvent molecules around fullerene. Taking into account only Van der Waals interaction, MDS data predict the existence of such shell (first coordination shell in Fig. 6). Let us assume that only the first coordination sphere can be reliably resolved in the SLD profile with $\rho_1 = 1.41 \times 10^{10}$ cm^{-2} (i.e., only $\rho_2 = \rho_s$). In accordance with (9) the corresponding model (*model 5*) gives higher $R_g = 3.93$ Å, which is, on the one hand, in perfect agreement with the experimental value. However, the model curve over the whole q interval differs systematically from the experimental scattering at large q values (Fig. 7). This means that the concept of a single solvation shell can hardly fit the experimental SANS data. At last, it should be mentioned that the homogeneous approximation to the fullerene molecule with the constant density $\rho_0 = 60 b_C / (4/3 \pi R_0^3) = 4.41 \times 10^{10}$ cm^{-2} in the multishell profile does not give reliable fits showing significant systematic deviations from the experimental data.

To reconcile the experimental data at the Guinier region and at the whole q interval the existence of small fullerene clusters can be considered. It is reasonable to assume that some fraction of dissolved fullerene molecules, α, is in dimers. In this approximation (*model 6*) Eq. (8) is transformed to

$$I(q) = nF^2(q)(1 + \alpha \sin(2qR_0)/(2qR_0)). \quad (10)$$

The parameter α includes also particles in close-packed trimers and tetramers (tetrahedrons), where the distance between monomers is equal to $2R_0$. Equation (10) is fitted to the experimental curve in Fig. 7 by varying α and R_0. The obtained α parameter takes a reasonable value of around 0.13 ± 0.04; while the resulting fullerene radius, $R_0 = (6.1 \pm 0.2)$ Å, corresponds well to the value obtained in MDS.

IV. CONCLUSION

To summarize, no indication of the equilibrium cluster state of C_{60} (with the cluster size below 60 nm) is revealed in the SANS experiments from C_{60}/CS_2 solutions, when the solutions are prepared in equilibrium conditions. Several scattering models of fullerene C_{60} in CS_2 are considered. Despite the fact that MDS resolves two density fluctuation shells (each 3 Å thick) of the solvent around the fullerene molecule in CS_2, yet the modeling of the scattering curves does not show any significant contribution of these shells in the scattering. Instead, the introduction of small stable clusters, such as dimers (particle number fraction about 0.1), makes the model to be more consistent with the experimental data; and at the same time good agreement is seen with respect to the partial volume of C_{60} in CS_2 $(690 \pm 4$ Å$^3)$ found in MDS.

[1] R. S. Ruoff, D. S. Tse, R. Malhotra, and D. C. Lorents, J. Phys. Chem. **97**, 3379 (1993).
[2] M.V. Korobov and A.L. Smith, in *Fullerenes: Chemistry, Physics, and Technology*, edited by K. M. Kadish and R. S. Ruoff (Wiley, New York, 2000), pp. 53–90.
[3] V. N. Bezmel'nitsyn, A. B. Eletskii, and M. B. Okun, Phys. Usp. **41**, 1091 (1998).
[4] M. V. Avdeev, T. V. Tropin, and V. L. Aksenov, "Models of fullerene cluster formation in solutions," Russian J. Phys. Chem. A (in press).
[5] A. Mrzel, A. Mertelj, A. Omerzu, M. Copic, and D. Mihailovic, J. Phys. Chem. **103**, 11256 (1999).
[6] M. Alfe, B. Apicella, R. Barbarella, A. Bruno, and A. Ciajolo, Chem. Phys. Lett. **405**, 193 (2005).
[7] S. Nath, H. Pal, and A. V. Sapre, Chem. Phys. Lett. **327**, 143 (2000).
[8] S. Nath, H. Pal, D. K. Palit, A. V. Sapre, and J. P. Mittal, J. Phys. Chem. B **102**, 10158 (1998).
[9] M. Beck, Pure Appl. Chem. **70**, 1881 (1998).
[10] T. Tomiyama, S. Uchiyama, and H. Shinohara, Chem. Phys. Lett. **264**, 143 (1997).
[11] K. Lozano, A. Gaspar-Rosas, and E. V. Barrera, Carbon **40**, 271 (2002).
[12] Q. Ying, J. Marecek, and B. Chu, Chem. Phys. Lett. **219**, 214 (1994).
[13] Q. Ying, J. Marecek, and B. Chu, J. Chem. Phys. **101**, 4 (1994).
[14] T. Rudalevige, A. H. Francis, and R. Zand, J. Phys. Chem. A **102**, 9797 (1998).
[15] G. Török, V. T. Lebedev, and L. Cser, Phys. Solid State **44**, 572 (2002).
[16] A. D. Bokare and A. Patnaik, J. Chem. Phys. **119**, 4529 (2003).
[17] T. V. Tropin, M. V. Avdeev, V. B. Priezzhev, and V. L. Aksenov, JETP Lett. **83**, 399 (2006).
[18] T. V. Tropin, M. V. Avdeev, and V. L. Aksenov Fullerenes, Nanotubes, Carbon Nanostruct. **16**, 616 (2008).
[19] M. V. Avdeev, T. V. Tropin, V. L. Aksenov, L. Rosta, and M. T. Kholmurodov, Surf. Invest. X-Ray Synchrotron Neutron Tech. **2**, 819 (2008).
[20] R. V. Honeychuck, T. W. Cruger, and J. Milliken, J. Am. Chem. Soc. **115**, 3034 (1993).
[21] R. S. Ruoff, R. Malhotra, D. L. Huestis, D. S. Tse, and D. C. Lorents, Nature (London) **362**, 140 (1993).
[22] M. V. Korobov, A. L. Mirakyan, N. V. Avramenko, and G. Olofsson, J. Phys. Chem. B **103**, 1339 (1999).
[23] M. V. Korobov, A. L. Mirakyan, N. V. Avramenko, and G. Olofsson, J. Phys. Chem. B **102**, 3712 (1998).
[24] K. A. Affholter, S. J. Henderson, G. D. Wignall, G. J. Bunick, R. E. Haufler, and R. N. Compton, J. Chem. Phys. **99**, 9224 (1993).
[25] L. A. Girifalco, J. Phys. Chem. **96**, 858 (1992).
[26] C. Gripon, L. Legrand, I. Rosenman, and F. Boue, Fullerenes, Nanotubes, Carbon Nanostruct. **4**, 1195 (1996).
[27] Y. B. Melnichenko, G. D. Wignall, R. N. Compton, and G. Bakale, J. Chem. Phys. **111**, 4724 (1999).
[28] S. J. Henderson, Langmuir **13**, 6139 (1997).
[29] F. Migliardo, V. Magazu, and M. Migliardo, J. Mol. Liq. **110**, 3 (2004).
[30] T. Malaspina, E. Fileti, and R. Rivelino, J. Phys. Chem. B **111**, 11935 (2007).
[31] B. Jacrot, Rep. Prog. Phys. **39**, 911 (1976).

[32] W. Smith and T. R. Forester, J. Mol. Graphics **14**, 136 (1996).
[33] M. P. Allen and D. J. Tildesley, *Computer Simulation of Liquids* (Clarendon Press, Oxford, 1989).
[34] D. J. Tildesley and P. A. Madden, Mol. Phys. **42**, 1137 (1981).
[35] S. B. Zhu, J. Lee, and G. W. Robinson, Mol. Phys. **65**, 65 (1988).
[36] B. M. Powell, G. Dolling, and B. H. Torrie, Acta Crystallogr., Sect. B: Struct. Crystallogr. Cryst. Chem. **38**, 28 (1982).
[37] W. I. F. David, R. M. Ibberson, J. C. Matthewman, K. Prassides, T. J. S. Dennis, and J. P. Hare, Nature (London) **353**, 147 (1991).
[38] K. Hedberg, L. Hedberg, D. S. Bethune, C. A. Brown, H. C. Dorn, R. D. Johnson, and M. Devries, Science **254**, 410 (1991).
[39] W. Krätschmer, L. D. Lamb, K. Fostiropoulos, and D. R. Huffman, Nature (London) **347**, 354 (1990).
[40] T. Freltoft, J. K. Kjems, and S. K. Sinha, Phys. Rev. B **33**, 269 (1986).
[41] J. S. Pedersen, D. Posselt, and K. Mortensen, J. Appl. Crystallogr. **23**, 321 (1990).
[42] E. P. Kozlova, Yu. M. Ostanevich, and L. Cser, Nucl. Instrum. Methods **169**, 597 (1980).
[43] D. I. Svergun, J. Appl. Crystallogr. **25**, 495 (1992).
[44] L. A. Feigin and D. I. Svergun, *Structural Analysis by Small-Angle X-Ray and Neutron Scattering* (Plenum, New York, 1987).
[45] O. Steinhauser and M. Neumann, Mol. Phys. **37**, 1921 (1979).
[46] S. Yamamoto, Y. Ishibashi, Y. Inamura, Y. Katayama, T. Mishina, and J. Nakahara, J. Chem. Phys. **124**, 144511 (2006).
[47] D. M. Lockwood and P. J. Rossky, J. Phys. Chem. B **103**, 1982 (1999).
[48] M. V. Avdeev, I. A. Bodnarchuk, V. I. Petrenko, Kh. T. Kholmurodov, and S. P. Yaradaikin, Russian J. Phys. Chem. A **83**, 1129 (2009).